Enhancing the Sustainability of Concrete Mixes Utilizing Supplementary Cementitious Materials in Renewable Energy Buildings

Arjan Fakhrulddin Abdullah
Technical Engineering College, Northern Technical University (NTU), Kirkuk, Iraq
arjan2006@ntu.edu.iq

Nabaz Yassen Ezuldin
Technical Engineering College, Northern Technical University (NTU), Kirkuk, Iraq
nabaz.shexani@ntu.edu.iq

Inas Mahmood Ahmed
Technical Engineering College, Northern Technical University (NTU), Kirkuk, Iraq
inas.mahmood@ntu.edu.iq

Zainab Al-Khafaji
Department of Civil Engineering, Faculty of Engineering and Built Environment, Universiti Kebangsaan Malaysia, 43600 UKM Bangi, Selangor, Malaysia | Imam Ja'afar Al-Sadiq University, Qahira, Baghdad, Iraq
p123005@siswa.ukm.edu.my (corresponding author)

Received: 25 June 2025 | Revised: 20 July 2025 | Accepted: 14 August 2025

 DOI: https://doi.org/10.48084/etasr.12936

ABSTRACT

The growing emphasis on sustainable infrastructure has increased interest in Geo-Polymer Concrete (GPC) as an eco-friendly alternative to Ordinary Portland Cement (OPC). This study evaluates the mechanical performance of GPC incorporating binary combinations of Supplementary Cementitious Materials (SCMs), specifically Ground Granulated Blast Furnace Slag (GGBS), fly ash, and metakaolin. Four mixes were developed and tested for compressive, splitting tensile, and flexural strength at 7 and 28 days. The blend of slag and fly ash (G1) exhibited superior strength characteristics, achieving 41 MPa in compression, 2.75 MPa in tensile strength, and 3.85 MPa in flexural strength at 28 days. The One-way Analysis of Variance (ANOVA) confirmed statistically significant variations between the mixes. The correlation analysis revealed strong linear relationships between the compressive strength and both tensile (R = 0.93) and flexural strength (R = 0.98), suggesting that the compressive strength may serve as a practical predictor in the early-stage mix design. The enhanced performance of slag-based mixes is attributed to the improved geo-polymer gel formation and matrix densification. These findings support the use of SCM-based GPC as a sustainable and high-performance material for renewable energy infrastructure, contributing to reduced carbon emissions and more efficient resource utilization in the construction sector.

Keywords-renewable energy; sustainable material; GGBS; eco-friendly material; supplementary cementitious materials

I. INTRODUCTION

Concrete remains an indispensable and resource-efficient material within the construction industry, offering structural longevity and adaptability across a broad range of applications. Its ubiquity is evidenced by its global usage, ranking second only to water in terms of the total consumption [1]. In 2021, approximately 4.1 billion tons of cement were produced globally, supporting an estimated annual concrete usage nearly sevenfold higher [2, 3]. However, the significant environmental burden associated with conventional concrete production—particularly the manufacture OPC—is increasingly under scrutiny. The cement industry is responsible for nearly 7%–8% of total anthropogenic CO_2 emissions, primarily due to

calcination processes and high energy demands [4]. In addition, the unsustainable extraction of natural aggregates and freshwater exacerbates the ecological degradation. To address these challenges, extensive research efforts have been directed toward developing GPC, a class of low-carbon binders derived from aluminosilicate precursors activated by alkaline solutions [5, 6]. GPC systems commonly incorporate SCMs [7], such as GGBS [8, 9], fly ash, and metakaolin, which significantly enhance both the mechanical performance and durability of concrete while substantially reducing its carbon footprint [10].

The use of GPC is particularly advantageous in sustainable infrastructure for renewable energy systems, involving wind turbine bases, hydroelectric dam linings, and the structural components of photovoltaic farms, where high compressive, flexural, and tensile strengths are required [11]. Geo-polymers, often referred to as third-generation binders following lime and OPC, are amorphous alkali aluminosilicate networks synthesized through the activation of solid aluminosilicate sources. These involve natural minerals, such as kaolinite and feldspar, as well as industrial by-products, including fly ash, metallurgical slags, and mining residues. The reactivity of these precursors is strongly influenced by their mineralogical composition, particle fineness, and glass content. Typical activators involve sodium hydroxide (NaOH), potassium hydroxide (KOH), sodium silicate (Na_2SiO_3), and potassium silicate (K_2SiO_3). Although KOH has a higher intrinsic alkalinity, NaOH is generally more effective in dissolving the silicate and aluminate species, thereby promoting the formation of geopolymer gel. The optimal performance of geo-polymer binders depends on a meticulous selection of raw materials, a precise mix design, and tailored processing parameters that suit specific structural and environmental requirements.

The integration of SCM-based GPC in renewable energy projects supports the carbon reduction, energy efficiency, and Sustainable Development Goals (SDGs). Utilizing industrial byproducts in concrete can enhance the lifespan and performance of renewable energy infrastructure while reducing the environmental impact, ensuring a more sustainable future. The increasing global need for sustainable urbanization has generated interest in integrating renewable energy solutions into the urban infrastructure design. The transition from fossil fuel-dependent systems to renewable energy sources is essential as the urban areas face increasing challenges related to energy consumption, greenhouse gas emissions, and resource availability. Urban areas are essential for energy sustainability. They use more than 75% of the global energy and generate 70% of the carbon dioxide emissions [12]. The advent of economic globalization and the spread of economic regions has resulted in a significant increase in the global energy and resource consumption, averaging an annual growth rate of 2.2%, while the construction industry accounts for 36% of the world's total energy consumption, making it the most energy-intensive sector [13]. Although fly ash–GGBS geo-polymer mixes have received considerable attention, there are significant knowledge gaps. For instance, authors in [14] demonstrated the influence of activator concentration and curing regimes on the mechanical properties, yet their study varied both NaOH molarity and heat curing simultaneously, making it difficult to isolate the individual effects on strength and microstructure. Similarly, while broad research indicates that GGBS replacement improves the compressive strength, they also reveal that such benefits are less pronounced in the splitting tensile and flexural strengths—highlighting an incomplete understanding of the multilateral strength behavior [15]. Furthermore, authors in [16] acknowledge significant challenges in standardizing the mix design, curing conditions, and performance metrics. Finally, research also emphasizes environmental and industrial-scale constraints—such as the scalability of the curing protocols and the cost-effectiveness of the activator dosages—which are seldom addressed in controlled lab experiments [14]. Collectively, these limitations underscore the need for a systematically controlled investigation that applies standardized mix designs, consistent curing environments, and direct comparisons of the mechanical and durability responses across binary SCM blends. This study aims to bridge those gaps by focusing on uniform experimental protocols and the statistical analysis of the key performance indicators.

Conventional structures employ fossil fuels, like coal, oil, and natural gas for their energy needs, which leads to environmental degradation and energy depletion. The concern for renewable energy sources, which are environmentally friendly, low-carbon, and sustainable, has grown in response to the climate change and other energy-related disasters [17]. Therefore, the integration of renewable energy sources into buildings has emerged as a significant factor in the energy transition of the conventional structures and a critical component of the urban planning and development strategies to mitigate the building sector's impact on the energy consumption and climate change [18].

One of the main objectives of the renewable energy is to reduce the dependency on fossil fuels and to mitigate the effects of the climate change. It is utilized to reduce the energy consumption and the associated greenhouse gas emissions, hence mitigating the environmental effect of the construction projects. Therefore, the development and use of renewable energy is essential for building the energy efficiency and emission reduction in order to promote the sustainable expansion of buildings in the energy sector and even globally, utilizing existing natural resources and techno-economic means [19].

Despite the growing body of research on GPC, most studies have focused on single-source SCMs, such as fly ash or slag in isolation, with limited emphasis placed on the synergistic effects of binary SCM combinations under standardized mix design and curing regimes. Moreover, the existing literature often overlooks the practical implications of inter-property relationships—such as compressive-to-tensile or compressive-to-flexural strength correlations—that could streamline predictive modeling in structural design. Additionally, few investigations have addressed the performance of binary SCM-based GPC, specifically in the context of renewable energy infrastructure, where the high durability, sustainability, and mechanical reliability are critical. These knowledge gaps hinder the optimized deployment of GPC in environmentally sensitive and performance-critical applications. Therefore, this study aims to bridge these gaps by systematically evaluating

the mechanical behavior of GPC incorporating binary blends of GGBS, fly ash, and metakaolin, and by establishing empirical strength correlations that can inform sustainable design practices in renewable energy projects.

The novelty of this study lies in its systematic evaluation of binary combinations of SCMs—namely, GGBS, fly ash, and metakaolin—within a unified GPC mix design framework. Unlike prior studies that typically assess individual SCMs or non-standardized blends, this work applies consistent alkaline activator proportions and curing protocols across all mixes to enable a direct performance comparison. Moreover, the research introduces a robust statistical framework, incorporating ANOVA and correlation analysis, to establish predictive relationships among the compressive, tensile, and flexural strengths—offering practical insights for performance-based mix design. The primary aim of this study is to investigate the mechanical performance of GPC prepared with binary SCM systems under controlled laboratory conditions, with a focus on the compressive strength, splitting tensile strength, and Modulus of Rupture (MOR) at both early (7-day) and mature (28-day) curing ages. By identifying the most effective SCM combination and quantifying the inter-property relationships, the study seeks to support the development of high-performance, low-carbon concrete solutions tailored for renewable energy infrastructure applications.

II. MATERIALS AND METHODS

A. Materials

1) Ground Granulated Blast Furnace Slag

GGBS is the refuse from blast furnaces utilized to produce iron. In the construction industry, GGBS is widely utilized as an additional cementitious ingredient. It enhances the sustainability, chemical resistance, workability, and durability of concrete when combined with Portland cement. The chemical and physical properties are presented in Tables I and II.

2) Fly Ash

Fly ash is a fine particulate byproduct generated from burning pulverized coal in electric power plants. It primarily consists of calcium oxides, iron, aluminum, and silicon. Incorporating fly ash into concrete reduces the environmental footprint by repurposing industrial waste and lowering the demand for cement. The chemical and physical properties of fly ash are illustrated in Tables I and II.

3) Metakaolin

Kaolinite is an inorganic clay; its chemical composition is $Al_2Si_2O_5(OH)_4$. Metakaolin is a dehydroxylated form of the clay mineral kaolinite associated with the reaction. Between 100°C and 200°C, kaolinite loses most of its adsorbed water, in the range from 500°C to 700°C; kaolinite is calcined by losing water by dihydroxylation. This process of converting kaolinite to Metakaolin involves removing the chemically bound hydroxyl ions, breaking the crystal structure, and generating a necessary amount of water to form the transition surface (reactive form of silica and amorphous alumina). The chemical and physical properties of Metakaolin are displayed in Tables I and II.

4) Cement

OPC of Class I has been utilized in this investigation for casting the control samples, which were kept in a dry condition without exposure to direct atmosphere. The physical and chemical properties of cement, based on Iraqi specification No.5/1984, are depicted in Tables I and II, respectively, [20].

TABLE I. PHYSICAL PROPERTIES

Material	Specific gravity	Specific surface area	Water absorption %	Dry loose unit weight kg/m^3	Sulfate amount (SO_3) (%)	Material finer than sieve 0.075 mm
FA	2.41	525 m^2/kg	-	-	-	-
GGBS	2.59	293 m^2/kg	-	-	-	-
Metakaolin	2.64	13.3 m^2/kg	-	-	-	-
Cement	2.59	374 m^2/kg	-	-	-	-
Coarse aggregate	2.68	-	1.15	1620	0.087	-
Fine aggregate	2.45	-	1.25	1793	0.073	1.85

TABLE II. OXIDE COMPOSITION OF CEMENT, FLY ASH, AND GGBS

Oxide composition	Content (%)			OPC
	Metakaolin	FA	GGBS	
CaO	3.37	1.580	30.10	62.6
Al2O3	39.5	22.13	8.770	5.20
SiO2	53.2	63.21	35.42	220
Fe2O3	0.92	7.150	1.990	3.40
MgO	0.25	2.390	6.930	2.40
SO3	0. 41	0.110	0.430	2.40
Loss of Ignition (LOI)	0.72	1.560	0.830	1.80

5) Sodium Silicate (Na_2SIO_3)

The concentration of sodium silicate (Na_2SiO_3) depends on the proportion of Na_2O to SiO_2, which determines the silicate modulus (SiO_2/Na_2O), and the amount of H_2O, which influences the viscosity and reactivity of the solution. A higher SiO_2/Na_2O proportion typically leads to a more viscous and less reactive solution, while a lower proportion results in increased alkalinity and reactivity.

6) Sodium Hydroxide (NaOH)

Sodium hydroxide (NaOH), available as 99% pure flakes, is dissolved in distilled water to prepare the required concentration for GPC. The molarity depends on the proportion of the flakes to water. As the dissolution is highly exothermic, the solution should be cooled by leaving it exposed to air for at least 2 h.

7) Superplasticizer

A commercially available superplasticizer is utilized as a high-range water-reducing admixture in all mixtures throughout this investigation. This admixture enhances both the water reduction and workability retention, enabling the production of high-performance concrete and/or highly workable concrete.

8) Aggregate Properties and Grading

The river gravel utilized in this investigation is 12.5 mm nominal size and was tested per ASTM C33-01, with its sieve analysis findings presented in Figure 1.

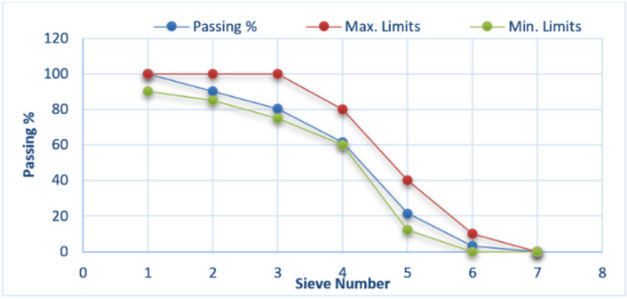

Fig. 1. Particle size distribution of coarse aggregate.

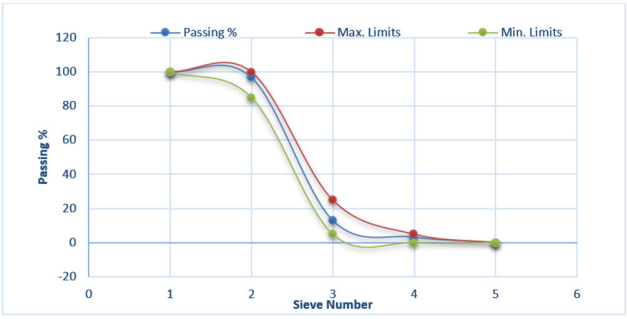

Fig. 2. Particle size distribution of fine aggregate.

Similarly, natural sand with a 4.75 mm max size was utilized as fine aggregate, conforming to the grading requirements of IQS No. 45/1984 – zone No. (3), with its sieve analysis findings exhibited in Figure 2. The particle size distribution curves indicate that both the fine and coarse aggregates possess well-graded profiles. This favorable gradation improves the packing density, reduces the voids, and facilitates the better bonding within the geo-polymer matrix, ultimately enhancing the compressive and flexural performance.

B. Mix Design for Geo-Polymer-Based Concrete (GPC)

The density of GPC incorporating fly ash, metakaolin, and slag at a 50% replacement level is comparable to that of conventional concrete, approximately 2400 kg/m^3. In this study, four different binder compositions were used and denoted as G0, G1, G2, and G3. The G0 mix contains 100% OPC (450 kg) as the sole binder, with no SCMs. In G1, the binder consists of 50% GGBS and 50% fly ash, with 225 kg of each material and no cement or metakaolin. The G2 mix includes 225 kg of GGBS and 225 kg of metakaolin, also at a 50%–50% ratio, with no cement or fly ash. Similarly, G3 comprises 225 kg of fly ash and 225 kg of metakaolin in equal proportions, excluding cement and GGBS. In all mixes, the coarse aggregate and fine aggregate quantities are constant at 1050 kg and 770 kg, respectively. To achieve optimal mechanical properties, critical mix design parameters were consistently controlled. These involved an alkaline liquid-to-binder proportion of 0.40, a Sodium Silicate-to-Sodium Hydroxide (SS/SH) proportion of 2.5, a sodium hydroxide molarity of 16M, a curing time of 24 h, a resting period of one day, and a superplasticizer dosage of 2.2%, with a fixed binder content of 450 kg across all mixes. The selected mix design, as presented in Table IV, exhibited enhanced mechanical performance, supported by the efficient role of the Alkaline Activator Solution (AAS) in promoting geo-polymerization. To ensure uniformity, the AAS was prepared one day prior to casting. During its preparation, sodium hydroxide was dissolved in water, releasing heat due to the exothermic nature of the reaction. Before mixing, all materials were conditioned to a surface-dry state and manually mixed for 4 to 5 min. The dry components—aggregates and binders—were then blended with the pre-prepared AAS along with a carefully measured amount of additional water to improve workability.

C. Statistical Analysis

To assess the substance of variation among the mechanical performance parameters of the various GPC mixtures, ANOVA was employed. This method assessed the variance between group means for compressive strength, splitting tensile strength, and MOR at both 7 and 28 days of curing. The application of ANOVA allows for the identification of statistically significant differences attributable to the changes in the binder composition across the experimental groups.

TABLE III. AMOUNT FOR GPC ACCORDING TO THE SPECIFIED MIX DESIGN

Symbol	Coarse agg. (kg)	Fine agg. (kg)	Binder percentage%	Cement (kg)	GGBS (kg)	Fly ash (kg)	Metakaolin (kg)	AA / binder proportion	SS/SH proportion	NaOH (kg)	Na_2SiO_3(kg)
G0	1050	770	100 %	450	---	---	---	---	---	---	---
G1	1050	770	50 %	---	225	225	---	0.40	2.5	45.75	114.25
G2	1050	770	50 %	---	225	---	225	0.40	2.5	45.75	114.25
G3	1050	770	50 %	---	---	225	225	0.40	2.5	45.75	114.25

III. RESULTS AND DISCUSSION

A. Compressive Strength

Figure 3 illustrates the compressive strength development of the GPC mixes G0-G3 at 7 and 28 days. The findings indicate that G1 (slag + fly ash) consistently exhibited superior performance, reaching a maximum compressive strength of 41 MPa at 28 days. This increment is primarily attributed to the synergistic pozzolanic and latent hydraulic reactions of fly ash and slag, which contribute to densified microstructures and long-term strength gains. G2 (slag + metakaolin) demonstrated moderate strength (34.5 MPa), suggesting that metakaolin supports early strength due to its highly reactive amorphous alumina and silica content, but does not sustain significant strength increases over time without the latent hydraulic contribution of fly ash. G3 (fly ash + metakaolin) recorded the lowest strength (29.6 MPa), likely due to the slower reactivity of fly ash and the lack of hydraulic activity in the absence of slag [2].

(a)

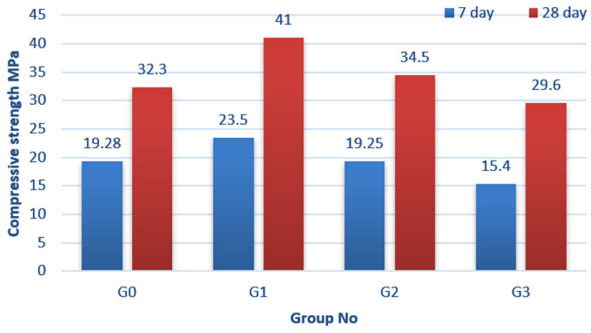

(b)

Fig. 3. Results of compressive strength test: (a) strength of different mixes, (b) specimen after failure under compressive load.

B. Tensile Strength

Figure 4 illustrates the splitting tensile strength values for the same mixes at both curing intervals. G1 again outperformed the other mixes, achieving a tensile strength of 2.75 MPa at 28 days. This strength improvement can be attributed to the strong interfacial transition zones and improved matrix integrity due to secondary Calcium-Alumino-Silicate-Hydrate (C-A-S-H) gel formation. G2 showed a tensile strength of 1.79 MPa, which is significantly higher than the reference mix G0 (1.35 MPa), suggesting that the slag's contribution to early-age bonding is more pronounced when paired with metakaolin. G3 had the lowest tensile strength (1.55 MPa), emphasizing that the fly ash and metakaolin combinations do not sufficiently improve the early tensile resistance without slag.

(a)

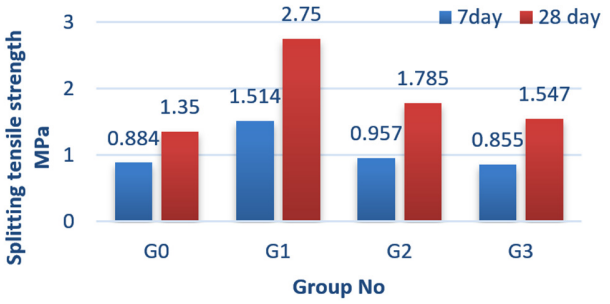

(b)

Fig. 4. Results of the split tensile strength test: (a) strength of different mixes, (b) specimen after failure under tensile load.

C. Modulus of Rupture (Flexural Strength)

Figure 5 presents the results of MOR, a critical indicator of a concrete mix's resistance to flexural stress. The G1 mix once again displayed superior behavior with a MOR of 3.85 MPa at 28 days. This enhancement is supported by the densified binder matrix and the interconnected network of C-A-S-H and N-A-S-H gels that effectively bridge the cracks under bending loads. G2 achieved a comparable but slightly lower strength (3.06 MPa), which still represents a significant improvement over G0 (2.58 MPa). G3 displayed a MOR of 2.78 MPa, better than the control but inferior to the slag-based mixes. The better performance of slag-containing mixtures aligns with the empirical observations in [24], where the mechanical superiority of slag-activated binders in flexural applications was emphasized due to their reduced porosity and enhanced microstructure continuity.

Renewable material concrete exhibits a higher MOR than normal concrete. This variation in MOR can be attributed to the unique characteristics of renewable concrete. The formation of strong covalent bonds during the curing process enhances the strength and durability of the material matrix. Additionally, renewable materials may experience lower creep and shrinkage compared to conventional concrete. This improved dimensional stability enables the material to better resist the flexural and bending forces.

(a)

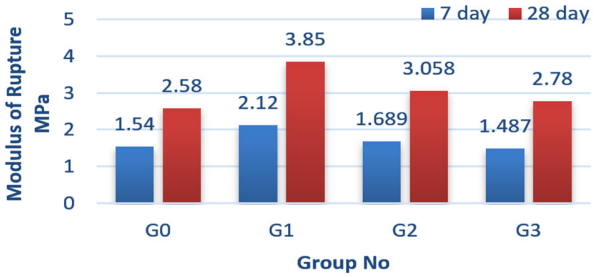

(b)

Fig. 5. Results of the MOR test: (a) strength of different mixes, (b) specimen after failure under flexural load.

D. Statistical Analysis Results

To evaluate the significance of the differences in the mechanical performance among the GPC mixtures, a one-way ANOVA was performed for the compressive strength, splitting tensile strength, and MOR at both 7 and 28 days. This statistical method identifies whether the observed variations in the strength parameters are due to the changes in the mix composition rather than random fluctuations. Table IV provides a statistical summary of the mechanical performance indicators of concrete, involving the compressive strength (*fc*), splitting tensile strength (*ft*), and MOR (*fr*), measured at 7 and 28 days of curing. Each parameter is described by key descriptive statistics: count, mean, standard deviation, minimum, first quartile (25%), median (50%), third quartile (75%), and max. At 7 days, the compressive strength (fc_7) exhibited a mean magnitude of 19.36 MPa with a standard deviation of 3.31 MPa, reflecting early-age development variability, commonly influenced by the hydration kinetics and binder characteristics [21, 22]. The splitting tensile strength (ft_7) showed a mean of 1.05 MPa, while the MOR (fr_7) averaged 1.71 MPa, indicating that tensile-related parameters develop at a relatively slower pace due to the delayed matrix continuity and microcrack propagation resistance [23]. At 28 days, the mean compressive strength (fc_{28}) increased significantly to 34.35 MPa, with an increased standard deviation of 4.87 MPa. This progression confirms the maturity-related strength enhancement consistent with the long-term hydration and pozzolanic reactions [22, 24]. Similarly, ft_{28} and fr_{28} recorded elevated mean magnitudes of 1.86 MPa and 3.07 MPa, respectively [25, 26]. Table V presents the findings of ANOVA applied to assess the statistical significance of the variation among four experimental groups in terms of early-age mechanical performance, specifically at 7 days of curing. The assessed parameters involve the compressive strength, splitting tensile strength, and MOR. Each test is accompanied by its respective *F*-value and associated *p*-value. The compressive strength at 7 days exhibits a highly significant variation among the groups, with an *F*-value of 25.97 and a *p*-value of 0.0022. This result, being well below the standard alpha level of 0.05, confirms that the observed differences in early compressive strength are statistically significant. This outcome can be attributed to the influence of the mix design variables (e.g., rubber content or treatment methods), which affect the hydration kinetics and the development of early mechanical properties [21, 22]. For the splitting tensile strength at 7 days, the ANOVA yields an *F*-value of 5.39 and a *p*-value of 0.059. Although this suggests a notable trend, it does not reach the conventional statistical significance at the 0.05 level. This could be due to the higher variability and sensitivity of the tensile properties at early ages, which are more affected by the microcracking and aggregate–matrix interface quality [23]. The MOR at 7 days also reveals statistically significant differences, with an *F*-value of 18.76 and a *p*-value of 0.0049. This indicates that MOR, like the compressive strength, is significantly influenced by the changes in the concrete composition or treatment conditions during the early stages of hydration. MOR development has been shown to be particularly responsive to the changes in aggregate gradation, binder type, and admixture content, which modulate the tensile zone cracking resistance in early curing periods [24, 25]. Figure 6 shows the correlation between the compressive strength and MOR of concrete at two distinct curing ages—7 and 28 days, revealing the age-dependent nature of their interrelationship. At 7 days, although the Pearson correlation coefficient (R = 0.91) suggests a strong linear association, the broad confidence interval observed in the regression model reflects substantial statistical variability, attributable to the incomplete hydration, microstructural heterogeneity, and early-age curing sensitivity. In contrast, the 28-day correlation (R = 0.93) exhibits a more coherent and statistically robust relationship, characterized by a well-defined regression trend and a narrowed confidence envelope. This improvement is attributed to the advancement of cement hydration and potential pozzolanic reactions, leading to a denser and more homogenous matrix that proportionally enhances both the compressive strength and MORs [27, 28], which underscores the enhanced predictability of the mechanical performance at extended curing periods [29, 30].

TABLE IV. DESCRIPTIVE STATISTICS AND CORRELATION

Parameters	Count	Mean	Standard deviation	Min	25%	50%	75%	Max.
fc_7	4.0	19.35750	3.30855834667205	15.40	18.2875	19.2650	20.3350	23.50
fc_{28}	4.0	34.35000	4.86518242206805	29.60	31.6250	33.4000	36.1250	41.00
ft_7	4.0	1.052500	0.3106450278587	0.855	0.87675	0.92050	1.09625	1.514
ft_{28}	4.0	1.857999	0.6206926238754	1.350	1.49775	1.66600	2.02625	2.750
fr_7	4.0	1.709000	0.287034260440573	1.487	1.52675	1.61450	1.79675	2.120
fr_{28}	4.0	3.066999	0.557586465641578	2.580	2.73000	2.91896	3.25600	3.850

TABLE V. ONE-WAY ANOVA FINDINGS

Parameters	*F*-value	*p*-value
Compressive strength (7d)	25.973125818641208	0.002229309959584 8123
Splitting Tensile strength (7d)	5.387169536124168	0.059365378500798 38
MOR (7d)	18.75621295155245 2	0.004924149509946 1826

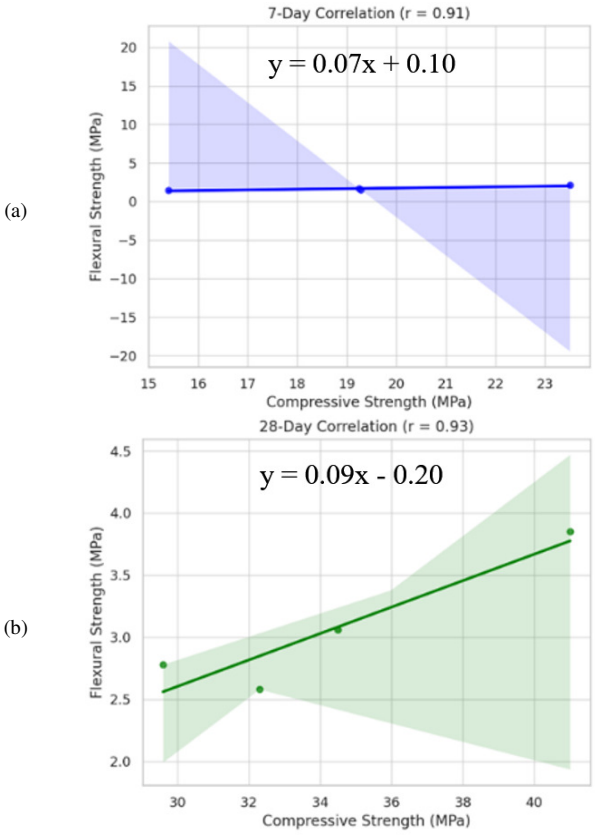

Fig. 6. Correlation between: (a) flexural strength and compressive strength, (b) compressive strength and MOR at 7 and 28 Days.

Figure 7 presents the correlation between the compressive strength and splitting tensile strength of concrete at 7 and 28 days of curing, which is displayed through linear regression plots accompanied by 95% confidence intervals. The left panel, corresponding to 7-day data, shows a moderately strong correlation (R = 0.88), indicating a positive but somewhat variable linear relationship. This variability, as evidenced by the broader confidence band, may be attributed to incomplete hydration and the early-age heterogeneity of the cement matrix, which affects the distribution of microcracks and internal bonding. In contrast, the right panel demonstrates a stronger correlation at 28 days (R = 0.93), accompanied by a narrower confidence region, signifying an improved statistical reliability and a more robust mechanical linkage. This enhancement in correlation is due to the progression of the hydration and pozzolanic activity, which leads to microstructural densification, improved interfacial transition zones, and a more homogeneous distribution of the load-bearing phases [28, 2]. The data confirm the well-documented empirical trend, according to which the tensile strength, while not directly proportional, can be reliably estimated from the compressive strength at later curing stages, a foundational concept for the models adopted in ACI 318 and Eurocode 2.

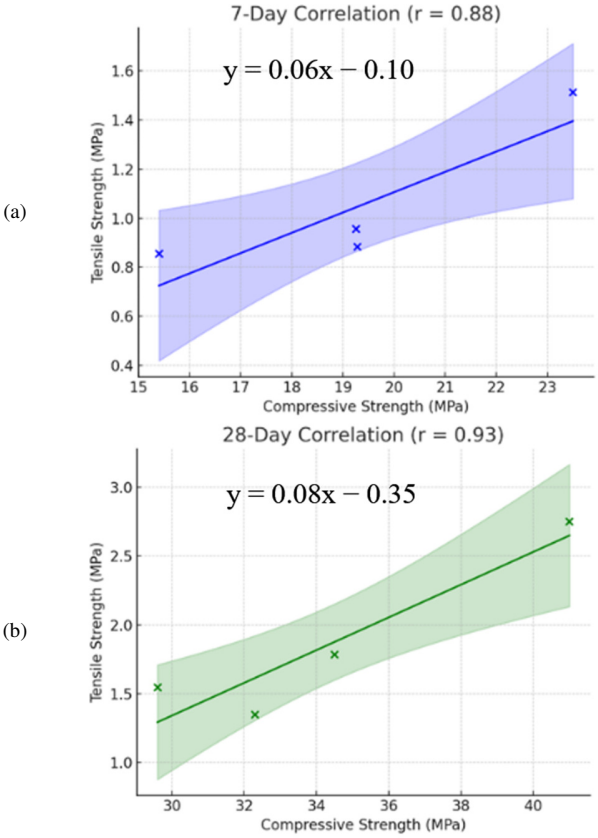

Fig. 7. Correlation between splitting tensile strength and compressive strength: (a) 7 days, (b) 28 days.

IV. CONCLUSION

This investigation examined the mechanical performance of GPC incorporating binary blends of supplementary cementitious materials—slag, fly ash, and metakaolin—under controlled curing conditions. Based on the compressive, splitting tensile, and Modulus of Rupture (MOR) tests at 7 and 28 days, the findings confirmed that the slag–fly ash mixture (G1) exhibited superior mechanical properties, achieving the highest compressive strength (41 MPa), tensile strength (2.75 MPa), and MOR (3.85 MPa) at 28 days. The slag–metakaolin combination (G2) showed a moderate strength development, while the fly ash–metakaolin mix (G3) demonstrated the lowest performance across all parameters. The One-way Analysis of Variance (ANOVA) validated the statistical significance of strength variation among the mixtures. Furthermore, the correlation analysis revealed a strong linear relationship

between the compressive strength and MOR (R = 0.98) and between the compressive and tensile strengths (R = 0.93), suggesting that the compressive strength can serve as a reliable indicator for estimating other mechanical parameters in GPC systems. These findings emphasize the critical role of slag in enhancing both the early-age and long-term strength through improved geo-polymerization kinetics and matrix densification.

While this study provides valuable insights into the mechanical performance of Geo-Polymer Concrete (GPC) incorporating binary combinations of Supplementary Cementitious Materials (SCMs), several limitations should be acknowledged. First, all experimental procedures were conducted under controlled laboratory conditions, which may not fully represent field environments where the temperature fluctuations, humidity variations, and curing inconsistencies can influence the material behavior. Additionally, the study focused exclusively on early (7-day) and standard (28-day) curing ages, without exploring the long-term performance, which is critical for assessing durability-related phenomena, such as carbonation, chloride penetration, and sulfate attack.

Furthermore, the study concentrated on mechanical properties—compressive, tensile, and flexural strengths—without addressing other essential performance criteria, such as shrinkage, creep, permeability, and resistance to thermal degradation or acid exposure. Microstructural analysis, such as Scanning Electron Microscopy (SEM) or X-Ray Diffraction (XRD), was not employed to verify the gel formation or matrix densification, which could enhance the understanding of the strength development mechanisms.

Future research should aim to extend this work by incorporating durability assessments, lifecycle performance modeling, and advanced microstructural characterization techniques. Additionally, investigating the behavior of GPC incorporating ternary SCM blends or hybrid reinforcement strategies under real environmental exposures and load conditions would contribute to developing robust, field-ready formulations. Finally, the integration of machine learning or optimization algorithms could be employed to predict the performance and reduce the trial-and-error burden in the mix design development for sustainable infrastructure applications.

REFERENCE

[1] Statista, *Global Cement Production 1995 to 2022*, Hamburg, Germany, 2023.

[2] P. J. M. Monteiro, S. A. Miller, and A. Horvath, "Towards Sustainable Concrete," *Nature Materials*, vol. 16, no. 7, pp. 698–699, July 2017, https://doi.org/10.1038/nmat4930.

[3] Z. A. Tunio, F. U. R. Abro, T. Ali, A. S. Buller, and M. A. Abbasi, "Influence of Coarse Aggregate Gradation on the Mechanical Properties of Concrete, Part I: No-Fines Concrete," *Engineering, Technology & Applied Science Research*, vol. 9, no. 5, pp. 4612–4615, Oct. 2019, https://doi.org/10.48084/etasr.3046.

[4] F. Preston and J. Lehne, *Making Concrete Change: Innovation in Low-carbon Cement and Concrete*, London, UK: Chatham House, 2018.

[5] D. S. Grebenkov, "Depletion of Resources by a Population of Diffusing Species," *Physical Review E*, vol. 105, no. 5, May 2022, Art. no. 054402, https://doi.org/10.1103/PhysRevE.105.054402.

[6] Y. Wada, L. P. H. Van Beek, C. M. Van Kempen, J. W. T. M. Reckman, S. Vasak, and M. F. P. Bierkens, "Global Depletion of Groundwater Resources," *Geophysical Research Letters*, vol. 37, no. 20, Oct. 2010, Art. no. 2010GL044571, https://doi.org/10.1029/2010GL044571.

[7] N. Bheel, R. A. Abbasi, S. Sohu, S. A. Abbasi, A. W. Abro, and Z. H. Shaikh, "Effect of Tile Powder Used as a Cementitious Material on the Mechanical Properties of Concrete," *Engineering, Technology & Applied Science Research*, vol. 9, no. 5, pp. 4596–4599, Oct. 2019, https://doi.org/10.48084/etasr.2994.

[8] Z. S. Al-Khafaji *et al.*, "Impact of High Volume GGBS Replacement and Steel Bar Length on Flexural Behaviour of Reinforced Concrete Beams," *IOP Conference Series: Materials Science and Engineering*, vol. 1090, no. 1, Mar. 2021, Art. no. 012015, https://doi.org/10.1088/1757-899X/1090/1/012015.

[9] Z. S. Al-Khafaji *et al.*, "The Impact of Using Different Ratios of Latex Rubber on the Characteristics of Mortars Made with GGBS and Portland Cement," *IOP Conference Series: Materials Science and Engineering*, vol. 1090, no. 1, Mar. 2021, Art. no. 012043, https://doi.org/10.1088/1757-899X/1090/1/012043.

[10] A. Fakhrulddin Abdullah, M. B. A.-D. Abdul-Rahman, and A. Abbas Al-Attar, "A Review on Geopolymer Concrete Behaviour Under Elevated Temperature Influence," *Journal of Sustainability Science and Management*, vol. 19, no. 12, pp. 239–259, Dec. 2024, https://doi.org/10.46754/jssm.2024.12.014.

[11] P. Duxson, A. Fernández-Jiménez, J. L. Provis, G. C. Lukey, A. Palomo, and J. S. J. Van Deventer, "Geopolymer Technology: The Current State of the Art," *Journal of Materials Science*, vol. 42, no. 9, pp. 2917–2933, May 2007, https://doi.org/10.1007/s10853-006-0637-z.

[12] V. J. Reddy, N. P. Hariram, M. F. Ghazali, and S. Kumarasamy, "Pathway to Sustainability: An Overview of Renewable Energy Integration in Building Systems," *Sustainability*, vol. 16, no. 2, Jan. 2024, Art. no. 638, https://doi.org/10.3390/su16020638.

[13] L. Chen *et al.*, "Green Building Practices to Integrate Renewable Energy in the Construction Sector: A Review," *Environmental Chemistry Letters*, vol. 22, no. 2, pp. 751–784, Apr. 2024, https://doi.org/10.1007/s10311-023-01675-2.

[14] Deepmala Pandey, Rakesh Kumar Pandey, and R. K. Mishra, "Analysis of Fly Ash and GGBS-based Geopolymer Concrete under Different Curing Conditions," *Journal of Environmental Nanotechnology*, vol. 13, no. 4, pp. 72–79, Dec. 2024, https://doi.org/10.13074/jent.2024.12.243939.

[15] A. A. Mohammed, H. U. Ahmed, and A. Mosavi, "Survey of Mechanical Properties of Geopolymer Concrete: A Comprehensive Review and Data Analysis," *Materials*, vol. 14, no. 16, Aug. 2021, Art. no. 4690, https://doi.org/10.3390/ma14164690.

[16] S. Nagajothi, S. Elavenil, S. Angalaeswari, L. Natrayan, and W. D. Mammo, "Durability Studies on Fly Ash Based Geopolymer Concrete Incorporated with Slag and Alkali Solutions," *Advances in Civil Engineering*, vol. 2022, no. 1, Jan. 2022, Art. no. 7196446, https://doi.org/10.1155/2022/7196446.

[17] S. Zhang, P. Ocłoń, J. J. Klemeš, P. Michorczyk, K. Pielichowska, and K. Pielichowski, "Renewable Energy Systems for Building Heating, Cooling and Electricity Production with Thermal Energy Storage," *Renewable and Sustainable Energy Reviews*, vol. 165, Sept. 2022, Art. no. 112560, https://doi.org/10.1016/j.rser.2022.112560.

[18] K. Kaptan, S. Cunha, and J. Aguiar, "A Review: Construction and Demolition Waste as a Novel Source for CO2 Reduction in Portland Cement Production for Concrete," *Sustainability*, vol. 16, no. 2, Jan. 2024, Art. no. 585, https://doi.org/10.3390/su16020585.

[19] M. Yang *et al.*, "Circular Economy Strategies for Combating Climate Change and Other Environmental Issues," *Environmental Chemistry Letters*, vol. 21, no. 1, pp. 55–80, Feb. 2023, https://doi.org/10.1007/s10311-022-01499-6.

[20] *Iraqi Standard Specification for The Portland Cement* IQS-5, Central Organization for Standardization and Quality Control, Baghdad, Iraq, 2005.

[21] A. A. Hilal, "Microstructure of Concrete," in *High Performance Concrete Technology and Applications*, S. Yilmaz and H. B. Ozmen, Eds, London, UK: InTechOpen, Oct. 2016, pp. 3–24.

[22] G. C. Lee, T. S. Shih, and K. C. Chang, "Mechanical Properties of Concrete at Low Temperature," *Journal of Cold Regions Engineering*, vol. 2, no. 1, pp. 13–24, Mar. 1988, https://doi.org/10.1061/(ASCE)0887-381X(1988)2:1(13).

[23] B. Zhang, "Durability of Low-carbon Geopolymer Concrete: A Critical Review," *Sustainable Materials and Technologies*, vol. 40, July 2024, Art. no. e00882, https://doi.org/10.1016/j.susmat.2024.e00882.

[24] A. Petrella and M. Notarnicola, "Recycled Materials in Civil and Environmental Engineering," *Materials*, vol. 15, no. 11, June 2022, Art. no. 3955, https://doi.org/10.3390/ma15113955.

[25] *Building Code Requirements for Structural Concrete and Commentary (reapproved 2022),* ACI 318-19, American Concrete Institute, Farmington Hills, MI, USA 2019.

[26] D. A. Abrams, *Design of concrete mixtures*, Chicago, IL, USA: Structural Materials Research Laboratory, 1919.

[27] A. M. Neville, *Properties of Concrete: Standards Updated to 2002*, 4th ed. Harlow, UK: Pearson Education, 2006.

[28] S. Mindess, J. F. Young, and D. Darwin, *Concrete*, 2. ed. Hoboken, NJ, USA: Prentice Hall, 2003.

[29] *Building Code Requirements for Structural Concrete and Commentary,* ACI 318M-19, American Concrete Institute, Farmington Hills, MI, USA, 2019.

[30] *Test Method for Flexural Performance of Fiber-reinforced Concrete (using Beam with Third-point Loading)* C1609/C1609M-12, ASTM International, West Conshohocken, PA, USA, 2012.